

Fire Detection using Time Series Analysis of Source Temperatures

Y. R. Sivathanu* & L. K. Tseng

Thermal Sciences and Propulsion Center, School of Mechanical Engineering,
Purdue University, West Lafayette, IN 47907-1003, USA

(Received 8 October 1996; revised version received 7 April 1997; accepted 7 May 1997)

ABSTRACT

The evaluation of a near-infrared fire detector using standard test fires is presented. The spectral radiation intensities incident on the fire detector are continuously measured at two near-infrared wavelengths (900 and 1000 nm), and a time series of apparent source temperatures is obtained from these measurements. The power spectral density and the probability density function of the apparent source temperatures are sufficient to determine the presence of a fire in the vicinity of the detector. The detector can also indicate the presence of a fire in an adjoining room from the radiation which is incident on it due to reflections from common building materials. © 1998 Published by Elsevier Science Ltd.

1 INTRODUCTION

New fire detection concepts and algorithms are justified only if they improve upon existing ones with lower false alarm rates and greater sensitivity to starting fires. In addition, the detectors and signal processing instruments should be easy to operate and maintain, have high flexibility and be relatively inexpensive.¹ Currently residential fire detectors include optical smoke sensors, ionization smoke sensors and temperature sensors.²

Conventional smoke sensors utilize light scattering or smoke ionization measurements to detect a fire, while temperature sensors utilize thermocouple measurements. There are three disadvantages with conventional single-sensor detectors: (1) there is a significant time delay between the start of the fire and

* Author to whom correspondence should be addressed. Tel.: 765 494 9364; fax: 765 494 0530; e-mail: sivathan@ecn.purdue.edu.

the transport of the combustion products to the location where the detector is mounted; (2) in instances where there are impermeable barriers (such as smoldering inside walls), the fire is not easily detected even in advanced stages, and; (3) single-sensor detectors involve a high rate of false alarms due to changes in the operating environment. Combinations of smoke sensors and odor sensors which involve multiple fire signatures are less prone to false alarms.³ However, multiple sensors involve greater construction cost and increased complexity of signal processing hardware and software.

More recently, there has been increased interest in the use of radiation-emission sensors (flame detectors) as an alternative to smoke and heat sensors.⁴ The three major advantages of emission sensors are: (1) their ability to survey the entire room for fire initiation, (2) their fast response time, and (3) false signals can be readily distinguished since most fires are unsteady with unique frequency content, leading to unambiguous discrimination based on the power spectral density of the measured intensities.²

Single-channel flame detectors operate either in the ultraviolet (where solar radiation is totally absorbed by the earth's atmosphere) or in the infrared (where flame emission is primarily from hot CO₂) parts of the spectrum. Ultraviolet signals from flames are normally very low, leading to false alarms from indoor radiation sources such as incandescent lights, arc welding processes, etc. Therefore, ultraviolet sensors are limited to outdoor usage where interfering solar radiation is absorbed by the earth's atmosphere. Another disadvantage of ultraviolet flame detectors is that any contamination of the optical windows causes a significant loss of sensitivity for these detectors.

Infrared flame detectors are used for large indoor areas such as aircraft hangars and warehouses where direct solar radiation is minimal. Single-channel infrared detectors look for radiation emitted from hot CO₂ gases present in most flames at wavelengths around 2.7 or 4.4 μm . These single-channel detectors have precision band-pass optical filters in front of them to detect fires while successfully rejecting solar radiation. The major problem with single-channel detection is that since only one channel of information is present, the chances of false alarms are relatively high.^{3,4}

The false alarm problems present with single-channel detection can be partially alleviated by using two channels of information. Typically, two-channel flame detectors use one channel in the infrared (typically at 4.4 μm) to detect hot combustion products. The second channel is chosen above or below the 4.4 μm band where there is a high level of solar radiation coupled with low levels of flame radiation. The addition of the second channel is purely for the prevention of false alarms by rejecting interference (such as direct solar radiation) from a continuum source that does not have the ubiquitous 4.4 μm CO₂ band. Fire is still detected using the 4.4 μm infrared channel, and in cases where fire is present along with the interfering source, it might be difficult to

resolve the signal unambiguously.⁴ Further, highly luminous fires may go undetected if the detector is tuned to non-luminous fires. Commercial production of single-channel infrared flame sensors which are insensitive to solar radiation, or a combination of ultraviolet/infrared and even two-channel infrared flame sensors has been initiated for use in industrial applications.⁴

A fiber-optic fire sensor that uses correlation between radiation at two wavelengths spaced far apart in the visible to 2.0 μm wavelength band has recently been utilized to detect diesel fires.⁵ The fiber-optic fire sensor utilizes the high degree of correlation between the intensities at the two wavelengths to provide immunity to false alarm sources. However, details regarding the hardware of the fiber-optic fire sensor or the fire detection algorithm were not reported.

The two most distinguishing features of a natural fire, particularly a luminous one, are its apparent source temperature and the power spectral density of the radiation intensities emitted from it. Two-wavelength pyrometric measurements conducted in luminous pool and jet fires⁶⁻⁸ indicate that the peak temperatures within these fires are in the range of 1400 ± 300 K. The power spectral density of natural fires shows a wide range of frequency present in them. Based on the above, the objective of the present work was to characterize the near-infrared radiation intensities emanating from standard test fires, with a view to developing an effective fire detection algorithm.

2 EXPERIMENTAL METHODS

The principle of operation of the near-infrared fire detector is similar to the two-wavelength optical pyrometer used for determining soot volume fractions and temperatures in laboratory-scale fires.⁷ The spectral radiation intensity emitted by a source at any wavelength can be obtained from the equation of radiative transfer as

$$I_{\lambda} = \varepsilon_{\lambda} I_{\lambda b} \quad (1)$$

where $I_{\lambda b}$ is the blackbody intensity at the unknown source temperature T and ε_{λ} is its apparent spectral emissivity.

For fire detection, the exact temperature and the emissivity of the source is not of great importance. Rather, the existence of high temperatures in the vicinity of the detector is sufficient to indicate the presence of a fire. Therefore, the spectral emissivity of any radiation source (either direct or reflected) can be assumed to vary inversely with wavelength irrespective of its chemical composition, or the spectral reflectivity of intervening material. Using this assumption, the apparent temperature of any source, determined from the

measured spectral radiation intensities at two wavelengths can be defined as

$$T = \frac{hc}{k} \left(\frac{1}{\lambda_1} - \frac{1}{\lambda_2} \right) / \ln \left\{ \left(\frac{\lambda_2^6}{\lambda_1^6} \right) \left(\frac{I_{\lambda_2}}{I_{\lambda_1}} \right) \right\} \quad (2)$$

where h is Planck's constant, k is the Boltzmann constant, and c is the speed of light. The advantage of using two wavelengths close to one another is that the assumption of $1/\lambda$ dependence for the emissivity of the source does not introduce a very large error on the apparent source temperatures obtained using eqn. (2).

A schematic diagram of the near-infrared fire detector is shown in Fig. 1. The fire detector consists of 90° view angle optics that collect and collimate the radiation intensity incident on it. The collimated radiation intensity is split into two parts which are incident on two photo-multiplier tubes (PMTs) with narrow-band-pass filters (10 nm FWHM) centered at 900 and 1000 nm in front of them. The output voltages of the two PMTs were monitored using an A/D board and a laboratory computer. These voltages were converted to spectral radiation intensities using calibration constants obtained with a reference blackbody (Infrared Industries) maintained at 1100 K.

The peak spectral radiation intensities in typical luminous fires such as acetylene and ethylene are at approximately 1500 nm.⁹ The intensities at 1000 nm are approximately a factor of three or four lower than at 1500 nm.⁹ However, there are three advantages to utilizing the spectral radiation intensities at 900 and 1000 nm rather than in the infrared regions to obtain apparent source temperatures: (1) near-infrared fire detectors are less expensive, more sensitive and less prone to degradation than infrared detectors, (2) the sensitivity of the two-wavelength pyrometric technique to temperature is more when the wavelengths are close together and well shifted from the

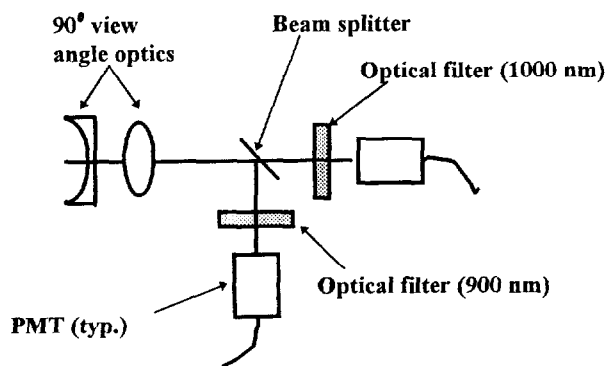


Fig. 1. Schematic diagram of the near-infrared fire detector.

peak of the Planck function, and (3) building materials are much more reflective at 900 and 1000 nm than at 1500 nm, making detection of reflected radiation easier. The lower sensitivity of the infrared detectors could be alleviated to some extent by utilizing broader bandwidth optical filters in lieu of the 10 nm filter used here. However, the detector will have higher false alarm rates due to the lower rejection of environmental radiation. For the characterization studies reported in the following, the choice of 900 and 1000 nm wavelengths is close to the optimal, providing both a higher sensitivity to temperatures and an increased immunity to false alarms.

The spectral radiation intensities at 900 and 1000 nm incident on the two photomultiplier tubes were measured at 500 Hz for the open and 100 Hz for the smoldering fires, respectively. From the spectral radiation intensities, a time series of apparent source temperatures was obtained using eqn. (2). The time series of spectral radiation intensities and apparent source temperatures were analyzed to obtain their probability density functions (PDFs) and power spectral densities (PSDs).

Fire detectors commonly used in residential and commercial buildings are tested using six standard fires specified in the European Committee for Standardization¹⁰ (CEN) guidelines. Five of these standard fires are luminous. The sixth one is a non-luminous alcohol fire which cannot be detected by the present fire detector. The near-infrared radiation characteristics of the five luminous fires were studied to develop an effective fire detection algorithm.

A brief description of the five test fires is included in the following section. Some of the dimensions of the fires specified in the CEN¹⁰ guidelines were scaled down so as to be able to accommodate them in our laboratories. The open cellulosic fire (designated TF1 in the CEN¹⁰ guidelines) consisted of seven stacks of beechwood sticks arranged to form a wooden crib. Each stack consisted of three beechwood sticks of dimensions 1 cm × 2 cm × 25 cm. The beechwood sticks were arranged in a cross-layer pattern to form a square wooden crib 250 mm on each side. The wooden crib fire was ignited with 5 cm³ of methylated spirit placed at the center.

The smoldering pyrolysis fire (designated TF2) consisted of 24 dried beechwood sticks arranged along the 12 radii of a grooved hot plate 220 mm in diameter. The beechwood sticks were 1 cm × 2 cm × 3.5 cm, and the hot plate was powered using a variable voltage controller so as to reach a temperature of 600°C in 11 min. The wood smolders at approximately 8 min. The radiation from the hot plate is very high and therefore a radiation shield was used to prevent the detector from directly viewing the hot plate. During the characterization tests, which lasted approximately 3 min, a flame was not present.

The glowing smoldering fire (designated TF3) consisted of 90 cotton wicks, 80 cm long, fastened by a wire ring 10 cm in diameter at one end. To maintain a cylindrical shape for the cotton wicks, they were wetted with water and

allowed to dry in a current of air, while a small tension was applied at the other end. The cotton wicks were ignited using a propane torch. The flames were put out immediately after ignition, and the cotton wicks continued to glow for a long time.

The open plastics fire (designated TF4) consisted of three mats of soft polyurethane foam stacked one on top of another. The mats were 15 cm in diameter and 25 mm in height. The polyurethane foam was not treated with any flame retarding additives, and therefore was very flammable. The bottom mat was ignited at one corner and the flame spreads very rapidly, with the entire fuel being consumed in approximately 1 min.

The liquid fire (designated TF5) consisted of an n-heptane pool fire stabilized on a water-cooled 15 cm diameter stainless-steel burner. The height of the stainless-steel burner was 10 cm, and the flames were stabilized with a lip height of 10 mm. The heptane pool fire reached a steady-state operating condition in approximately 3–4 min.

The near-infrared fire detector was placed at distances of 1 and 3 m from the center of the test fires. These two distances were chosen to vary the radiation intensities incident on the detector by approximately one order of magnitude, thereby providing a sensitivity analysis for the fire detection algorithm.

3 RESULTS AND DISCUSSION

The PDFs of spectral radiation intensities at 900 and 1000 nm (with the detector at 1 and 3 m from the center of the heptane pool fire, TF5) are shown in the top and bottom panel, respectively, in Fig. 2. The PDFs are nearly Gaussian in shape. The radiation intensities incident on the detector during regular operation are expected to vary depending on the proximity of the fire. The values of the spectral radiation intensities incident on the detector at a distance of 3 m are an order of magnitude lower than when the detector is 1 m from the center of the pool fire. Therefore, a conventional low-end cut-off algorithm for fire detection would not be successful, especially when the background signal (fluorescent lamps, solar radiation, etc.) incident on the detectors can vary widely depending on illumination present in the room.

The near-infrared fire detector is based on a statistical analysis of the estimated or apparent source temperatures obtained from the spectral radiation intensities. The spectral radiation intensities at the two wavelengths were converted into apparent source temperatures using Eq. (2). The PDFs of apparent source temperatures obtained when the infrared fire detector is at distances of 1 and 3 m from the center of the pool fire are shown in the top and bottom panels, respectively, in Fig. 3. The PDFs of apparent source temperature are also Gaussian in shape. Despite the order of magnitude difference

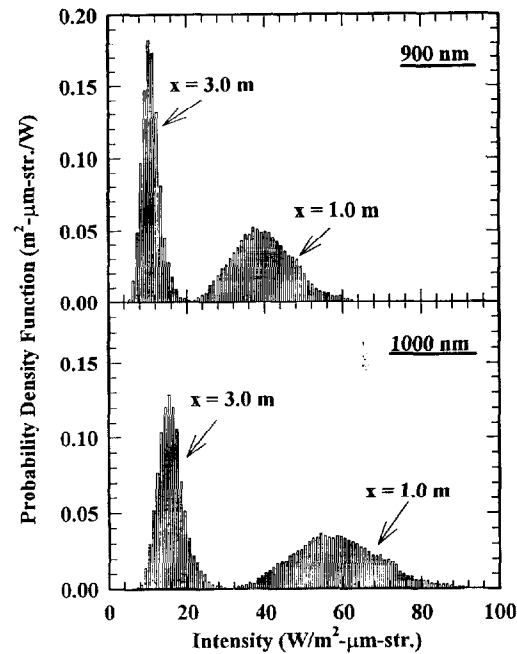


Fig. 2. The PDFs of spectral radiation intensities emanating from a heptane pool fire.

between the spectral radiation intensities incident on the fire detector, the PDFs of apparent source temperatures are limited to a narrow range near 1600 K.

The power spectral densities (PSDs) of apparent source temperatures obtained when the fire detector is at distances of 1 and 3 m from the center of the pool are shown in Fig. 4. The area under the PSD curve for any frequency range is proportional to the energy of the instantaneous fluctuations of the apparent source temperatures from the mean value. Most of the energy of the source temperature fluctuations is below 40 Hz irrespective of the distance of the fire from the detector.

The PDFs of spectral radiation intensities for all the test fires at a distance of 1 m from the detector are shown in Fig. 5. The wooden crib fire has the highest levels of radiation intensities emanating from it. The heptane pool fire has an order of magnitude lower radiation intensities emanating from it. The three open fires (TF1, TF4 and TF5) have much higher intensities than the two smoldering fires as expected. The smoldering cotton fire has two orders of magnitude lower intensities incident on the detector than the open wood fire, while the smoldering wood fire has three orders of magnitude lower intensities. The major reason for the much lower intensities of the smoldering

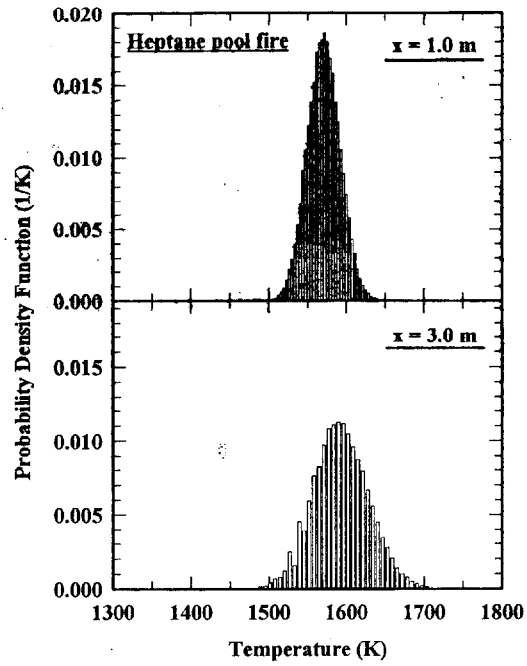


Fig. 3. The PDFs of estimated source temperatures from a heptane pool fire.

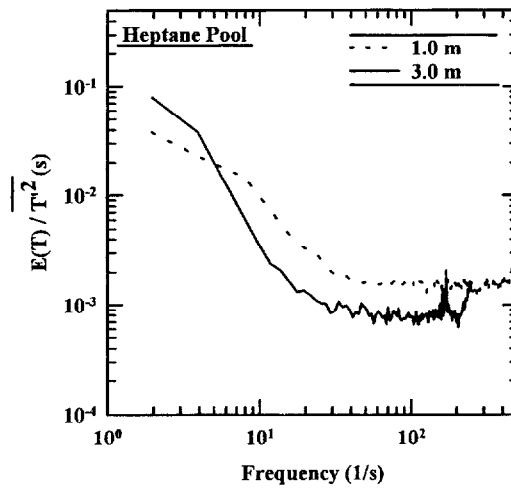


Fig. 4. The PSD of apparent source temperatures obtained from a heptane pool fire.

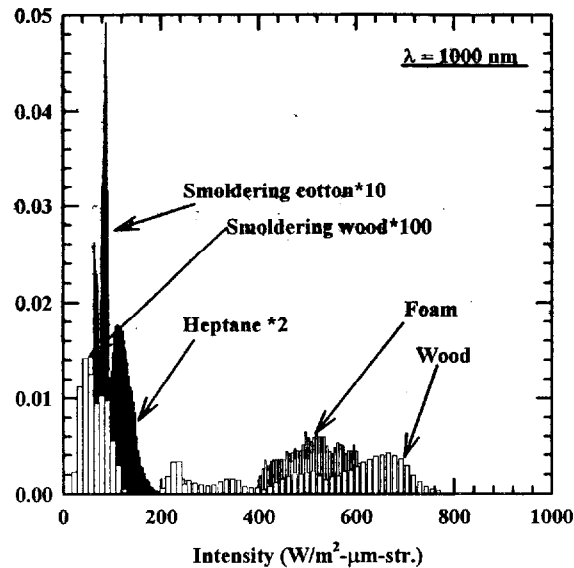


Fig. 5. PDFs of spectral radiation intensities from five test fires.

wood fire in comparison with that of the smoldering cotton fire is that most of the radiation emanating from the wooden chips propagate downward towards the burner surface. Since the radiation from the burner is shielded from the detector, only a small portion of the radiation emanating from the wooden fire is incident on the detector. In actual fire scenarios, the intensities from a wooden smoldering fire is expected to be at least as high as that of the cotton smoldering fire.

Depending on the proximity of the detector to the fire as well as the chemical composition of the fire, the intensities incident on the detector will vary widely. In addition, the background radiation incident on the detector can also vary depending on the illumination level present in the room. Conventional flame detectors have to account for this wide variation in the absolute radiation intensities emanating from these fires. Therefore, flame detectors operating on the principle of detecting absolute intensities at one or two fixed wavelengths and which are tuned to be very sensitive so as to detect the smoldering cotton fire will suffer from a high incidence of false alarms from natural sources such as sunlight, incandescent and fluorescent bulbs, etc.

The PDFs of apparent source temperatures obtained from the five test fires are shown in Fig. 6. Despite the three orders of magnitude difference in the absolute values of radiation intensities, all the test fires have an apparent source temperature that varies between 900 and 1800 K. The open wood,

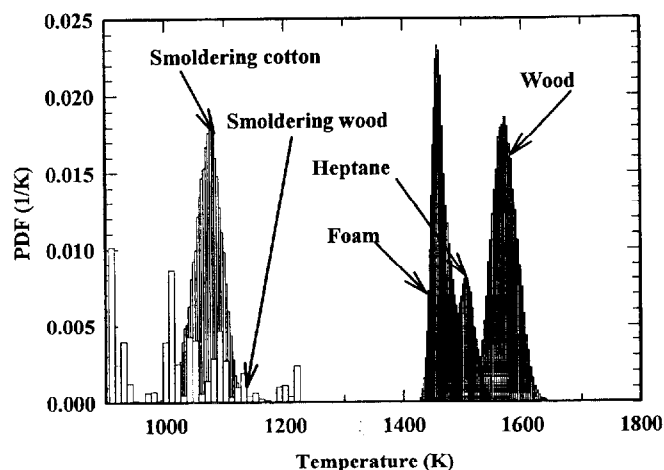


Fig. 6. PDFs of apparent source temperatures for the test fires.

plastic and heptane fires have apparent source temperatures that range from 1400 to 1700 K. The temperatures inferred from the spectral radiation intensities are biased towards the maximum temperatures present at any time in the flame. Even though parts of the flame may be at low temperatures, the peak temperature over the entire flame volume is rarely less than 1500 K.

The smoldering cotton and wood fires have much lower apparent source temperatures that range from 900 to 1200 K. The PDF of source temperatures obtained from the smoldering wood fire (TF2) is very noisy. The major reason for this is that the radiation intensities emanating from this fire are so low, that the SNR is low. In fact, the radiation intensities incident on the detector are close to the lower limit of detectability of the PMTs. However, the uncertainty in the estimated source temperatures is not of a major concern for the purpose of fire detection. Background solar radiation would provide a much higher source temperature (around 5800 K) since the ratio of intensities at 900 and 1000 nm are higher than from these luminous flames.

The power spectral densities (PSDs) of apparent source temperatures for the five fires are shown in Fig. 7. Most of the energy of the source temperature fluctuations for the open fires fall between 0 and 20 Hz and for the smoldering fires are between 0 and 5 Hz. The spectrum of white noise would be a flat line on this curve. Artificial light sources such as an incandescent or fluorescent lamp and AC noise would have a very high peak at 60 Hz and its multiples. A hot plate or solar radiation would have no fluctuations present in them. Therefore, using the PSDs of the apparent source temperatures provides us with another means of distinguishing accidental fires from the background illumination present in the room. The PDFs of apparent source temperatures

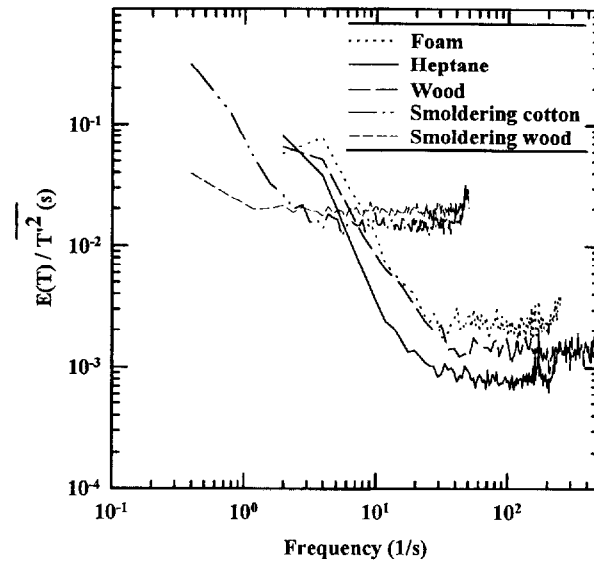


Fig. 7. PSDs of apparent source temperatures for the test fires.

inferred from the radiation intensities emitted by a tungsten filament lamp would be very close to 1500 K. Therefore, if only the PDFs of source temperatures were used in a detection algorithm, the detector would signal a fire in the presence of such lamps. To circumvent this problem, PSDs of source temperatures are also used in the fire detection algorithm.

For a random signal, the PSD will be flat over the frequency range of interest. Therefore, choosing a particular sampling frequency also dictates the area of the PSD curve below any specified frequency. For example, if the sampling frequency is 100 Hz, almost 80% of the area of the PSD for a random signal would be below 40 Hz. The test fires were sampled at different frequencies to obtain a good representation of their radiation signals. For the five test fires, the area under the PSD curve normalized by the area under the PSD curve for a random signal is shown in Fig. 8.

For four of the test fires, the area under the PSD curve for frequencies below 10 Hz is at least twice that of a random signal. For the smoldering wood fire, the SNR is very low and, consequently, the area under its PSD curve is not very different than that from a random signal. An appropriate sampling frequency for all the fires would be 100 Hz, with a low-pass filter applied at 50 Hz. The advantage of this sampling scheme would be the elimination of the 60 Hz signal from fluorescent lamps.

From the present data, two criteria for distinguishing fires from interfering sources has been chosen. The two criteria are: (1) at least 40% of the PDF of

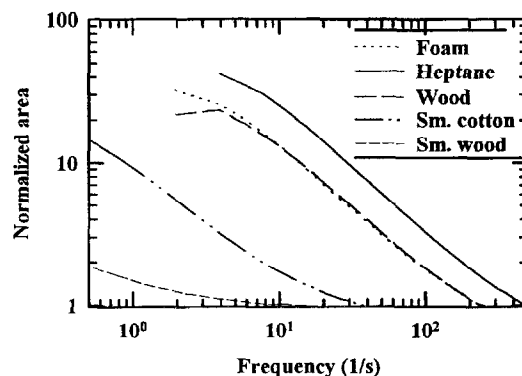


Fig. 8. Normalized area under the PSD curves for the test fires.

apparent source temperatures should be between 700 and 2500 K and (2) the area of PSD curve below 10 Hz should be at least 1.5 higher than that from a random signal. Currently, all the test fires other than the smoldering wood fire would satisfy the above two criteria. The second criteria requires a greater sensitivity of the detector. The first condition is important to detect sources of high temperatures in the immediate vicinity of the fire detector. The second condition is important to eliminate ambiguous signals originating from natural and artificial sources such as incandescent and fluorescent lamps, solar radiation reflected from building materials, natural gas burners and electric hot plates.

The near-infrared fire detector was then tested for continuous operation by switching on the detector and igniting the propane jet flame at arbitrary time intervals in the test room, either within its direct view (90° angle shown in Fig. 1) or outside it. The relative locations of the propane jet flame with respect to the fire detector are shown in Fig. 9.

The PDFs of apparent source temperatures from a propane/air diffusion flame when the radiation is direct as well as when it is reflected from a window pane or a brick wall are shown in Fig. 10. The intensities obtained from reflected radiation at 900 and 1000 nm are an order of magnitude lower than those obtained from direct radiation. Therefore, conventional fire detection algorithms (based on the absolute magnitude of intensities), which have to account for this variation, result either in decreased sensitivity or lower immunity to false alarms. The PDFs of apparent source temperatures obtained from the reflected radiation are shifted to higher values. This effect is caused by the preferential absorption of the longer wavelength (1000 nm) radiation by the window pane and the brick wall. However, the PDFs of apparent source temperatures shown in Fig. 10 are well within the criteria specified above.

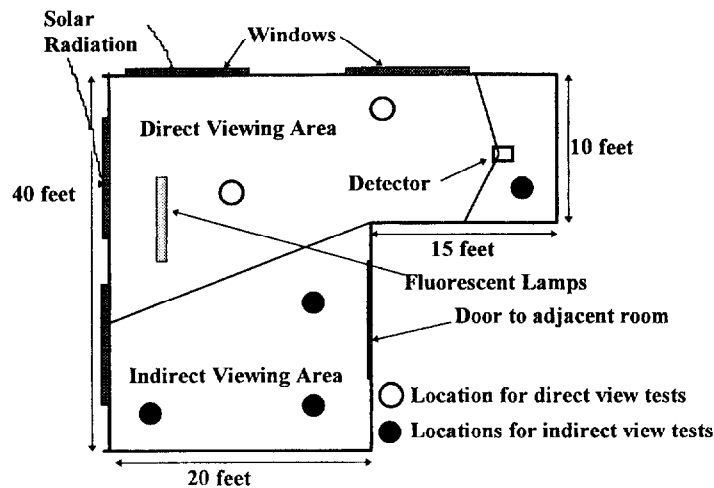


Fig. 9. Experimental arrangement for fire detection tests.

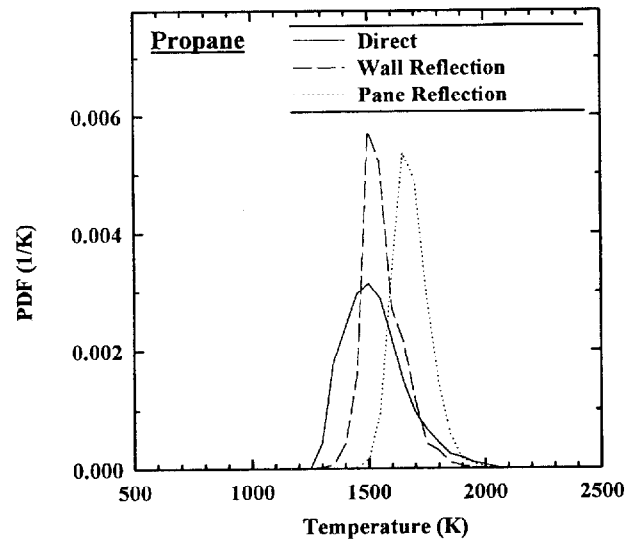


Fig. 10. PDFs of apparent source temperatures obtained from direct and reflected radiation.

The PSDs of apparent source temperatures from a propane/air diffusion flame when the radiation is direct as well as when it is reflected from a window pane or a brick wall are shown in Fig. 11. The time scales for radiation within most enclosures (distance traveled divided by the velocity of light) are extremely short, even with multiple reflections in comparison to the shortest

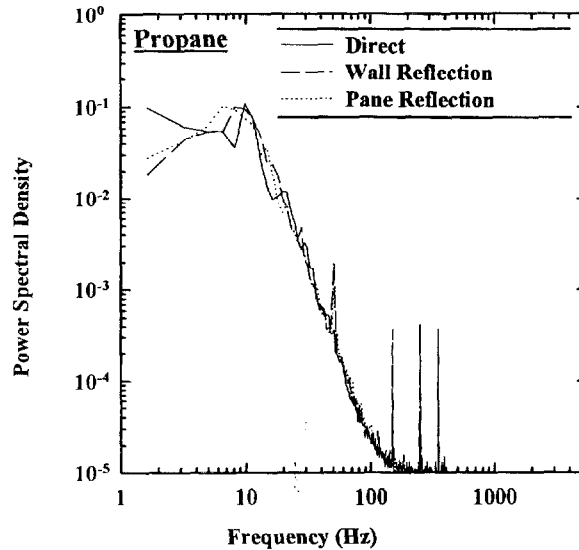


Fig. 11. PSDs of apparent source temperatures obtained from direct and reflected radiation.

turbulent time scales within the fire. Therefore, the PSDs for direct as well as reflected radiation are nearly identical as shown in Fig. 11. The much lower intensities obtained from the reflected radiation result in a lower SNR. Therefore, the PSDs for the reflected radiation show the discrete (60 Hz and its multiples) spectra obtained from the incandescent, and fluorescent lamps as well as from electrical noise in the power line.

Each time the test fire was ignited, the fire detector responded with a positive indication of fire within 30 s, irrespective of the location of the fire. This implies that the detector can operate successfully, even if the radiation intensities incident on the detector were obtained from reflections of intervening barriers. The radiation intensities incident on the detector from reflected radiation are an order of magnitude lower than those from direct radiation. Therefore, it might not be possible to detect the smoldering fires from reflected radiation. In addition, there were no instances of false alarms during the entire test period even when the background illumination was changed by switching on and off various fluorescent and incandescent lamps and closing and opening windows to allow more or less solar radiation to fall on the detector.

4 CONCLUSIONS

A near-infrared fire detector which operates on the principle of apparent source temperatures obtained from spectral radiation intensity measurements

at two near-infrared wavelengths was evaluated in this study. A detection algorithm capable of indicating the presence of fire in the vicinity of the detector based on the probability density function and power spectral density of apparent source temperatures was developed. The detector is also effective for detecting fires that are not in its direct view and in the presence of interference from natural and artificial sources.

ACKNOWLEDGEMENTS

This work was performed under the sponsorship of the U.S. Department of Commerce, National Institute of Standards and Technology under Grant No. 60NANB5D0113 with Dr William Grosshandler serving as the Federal Program Officer.

REFERENCES

1. Luck, H. O., Dedicated detection algorithms for automatic fire detection. *Proc. 3rd Int. Symp. on Fire Safety Science*, 1992, pp. 135–48.
2. Grosshandler, W. L., An assessment of technologies for advanced fire detection. In *Heat and Mass Transfer in Fire and Combustion Systems*, Vol. **HTD-223**, ASME, New York, 1992, pp. 1–9.
3. Okayama, Y., Ito, T. & Sasaki, T., Design of neural net to detect early stages of fire and evaluation by using real sensors' data. In *Proc. 4th Int. Symp. on Fire Safety Science*, 1994, pp. 751–9.
4. Middleton, J. F., Flame detectors. *9th Int. Conf. on Automat. Fire Detection*, AUBE-89, Duisburg, Germany, 1989, pp. 143–54.
5. Wetzork, J. M., Kern, M. T. & Shamrodola, K. A., Fiber optic fire sensor. In *Fiber Opt. and Laser Sensors X*, *SPIE*, **1795**, 1992, pp. 280–5.
6. Y. R. Sivathanu & G. M. Faeth, Temperature/soot volume fraction correlations in fuel-rich region of buoyant turbulent diffusion flames, *Combust. Flame* **81** (1990) 150–165.
7. Sivathanu, Y. R., Gore, J. P. & Dolinar, J. Transient scalar properties of strongly radiating jet flames, *Combust. Sci. Technol.* **76** (1991) 45–67.
8. Sivathanu, Y. R. & Gore, J. P., Simultaneous multiline emission and absorption measurements in optically thick turbulent flames, *Combust. Sci. Technol.* **80** (1991) 1–21.
9. Gore, J. P., A theoretical and experimental study of turbulent flame radiation. Ph.D. Thesis, Pennsylvania State University, PA, 1986.
10. CEN, Components of automatic fire detection systems: fire sensitivity test. *Part 9. European Committee for Standardization*, Brussels, 1982.